Technoscience Journal for Community Development in Africa 4 (2025) 119–127
ISSN 2659-0573

Research Article

Deformation and material removal mechanisms of nanometric cutting of silicon at different depths of cuts using molecular dynamics simulation

Tirimisiyu Olaniyan[1*], Peter Odedeyi[2], Victor Ejiofor[3]

[1]Department of Materials Science and Engineering, Kwara State University, Malete, Nigeria
[2]Centre for Advanced Design and Manufacturing, Mechanical Engineering Department, Faculty of Engineering and Design, University of Bath, England
[3]Department of Mechatronics Engineering, Nelson Mandela University, Port Elizabeth, South Africa.

Abstract: The diamond tool with a rake angle of zero has been rarely studied, and the cutting mechanism in ultraprecision machining of brittle materials, such as silicon, is not well understood due to the varying cutting parameters involved. The use of this tool was investigated through molecular dynamics simulation to examine the material removal mechanisms in silicon nanometric cutting at different depths of cut. Simulations were performed using the large-scale atomic/molecular massively parallel simulator with the Tersoff potential function Mechanisms of chip formation and material removal were analysed at three different depths of cut (2 nm, 3 nm, and 4 nm). The study reveals that the structural and phase transformations in silicon are caused by high-pressure phase changes and dislocation activity leading to chip formation and material removal. Machining at a lower depth of cut results in a machined surface with less subsurface damage. For all depths of cut, the material removal mechanisms operate in a ductile mode, except at 4 nm, where a combination of ductile and brittle (cleavage) modes is observed on the machined surface. To ensure a ductile machining mode with this tool geometry, the depth of cut should be significantly smaller than the cutting-edge radius of the diamond tool to achieve a high-quality surface finish.

Keywords: ductile mode machining, ultraprecision machining, brittle and hard materials, depth of cut, molecular dynamics

1. Introduction

Ultraprecision machining is a machining technique in which dimensional tolerance is achievable in the order of 0.01μm and that of surface roughness of 0.001μm (1nm) (Taniguchi, 1983). Among advanced manufacturing technologies, ultraprecision machining's role can't be ignored because parts with high accuracy, low subsurface damages, and improved surface quality are produced, and they meet the requirements of various applications such as electronics devices, optical systems, Information and Communication Technology (ICT), power devices, solar energy facilities, and others (Ikawa et al., 1991a; Ngoi & Sreejith, 2000; Shore & Morantz, 2012). Ultraprecision machining of materials of hard and/or brittle materials has gained popularity in the manufacturing industry for decades. The machining process technique that can produce components of good surface integrity with low surface roughness and/or low subsurface damage and requires one or no post-processing process, such as polishing, is referred to as a ductile regime machining process (Cai et al., 2007; Neo et al., 2012; Arif et al., 2013). However, the exact material removal mechanisms underlying ductile-regime machining of brittle and/or hard materials, such as silicon at the micro/nanoscale level,

* Corresponding author:
Email: tirimisiyu.olaniyan@kwasu.edu.ng

KWASU PRESS AND PUBLISHING

remain the subject of debate among researchers and machinists. The varying observations among experts in this research discipline are due to the complex nature of ultraprecision machining because there is a plethora of interplay processes involved. Such a process includes tool geometry, chip formation mechanism, stagnation effects, crystallographic and microstructural effects, tool wear, temperature-friction effects, machined surface properties, phase transformation, dislocation theory, constitutive material model, stress distribution, and so on (Venkatachalam, 2007). Unlike metals, materials such as advanced ceramics, semiconductors (e.g silicon), composites, and others are often referred to as brittle and/or hard materials due to their brittleness and hardness properties (Bifano et al., 1991). They have been used in many engineering applications: components in micro-electro-mechanical systems (MEMS) and nano-electro-mechanical systems (NEMS), optoelectronics devices, optical devices, ICT and so on (Ravindra et al., 2012). Their unique properties, such as wear resistance, high thermal strength, high strength, and hardness, have made them indispensable as engineering materials (Ebizuka et al., 2003). Various manufacturing techniques, such as laser machining, injection moulding, and others, are employed to incorporate these materials into devices like MEMS and NEMS. Where a complex shape of the components and better accuracy are required, precision/ultraprecision machining is mostly employed (Davies et al., 2003). Despite the unique properties of these materials compared to alloy metals, there are challenges in machining. These challenges are attributed to their high hardness and brittleness, in addition to their low fracture toughness (Ravindra et al., 2012; Agarwal et al., 2017;). Such challenges include tool wear leading to high production costs, poor material removal rate, poor surface finish, and others.

Single-crystal silicon is a material with different industrial applications, including large-scale integrated circuits as a semiconductor, infrared imaging or detection as an optical material, photovoltaic power, and photoelectrical sensors (Zhang et al., 2014). Silicon is a hard and brittle material, with a hardness in the range of 12 to 14GPa and a fracture toughness of 1 $MPa.m^{1/2}$. Therefore, it is categorised as a difficult-to-machine material. Numerous studies have been conducted on silicon that investigated its machining mechanism at the nanoscale using single-point demand turning, grinding, and scratching via ductile regime machining (Bifano et al., 1991; Lin et al., 2007; Ravindra et al., 2012; Wang et al., 2017; Xu et al., 2018; Z. Zhang et al., 2018). It has been established that machining at the nanoscale level involves complex phenomenal observations (Venkatachalam, 2007). These phenomena are also difficult to observe experimentally or theoretically in many cases (Komanduri & Raff, 2001). Much research has been carried out that reveals that molecular dynamics (MD) simulation is capable of investigating most of these phenomena such as chip formation mechanism, mechanism of dislocation, phase transformation, crystallographic orientation, friction, and so on (Ikawa et al., 1991b; Maekawa & Itoh, 1995; Cheng et al., 2003; Goel, 2013; Chavoshi, 2016a)). Tool geometry plays a significant role in the ultraprecision machining of materials. An investigation by Liu et al. (2021) reveals that machining at different negative rake angles could result in shear process, phase transition and extrusion process depending on the rake angle values. With the decrease of the rake angle (from –15˚ through to –60˚), the dominance of the cutting mechanism transits from shear to extrusion, and finally, no material removal would be observed (Liu et al., 2021). Nanometric cutting of single-crystal Ni_3Al using MD simulation shows that chip thickness decreased as the rake angle changed from positive (30˚) to negative (–30˚), and with an increase in rake angle, subsurface damage decreased (Feng et al., 2020). This research is a preliminary study to investigate how diamond tool geometry with a rake angle of 0˚ and clearance angle of –10˚ at different depths of cut affects the deformation and material removal mechanisms during ductile nanometric cutting of silicon using molecular dynamics simulation.

2. Materials and methods

2.1. Molecular dynamics methodology of nanometric cutting.

A molecular dynamics (MD) simulation model of a nanometric cutting of a single-crystal silicon workpiece and diamond cutting tool in a three-dimensional size was constructed, and its schematic diagram is illustrated in Figure 1. The computational parameters of the molecular dynamics simulations are given in Table 1.

Ensuring that the simulation is closer to the real cutting process, the workpiece (silicon) and the diamond cutting tool were set as deformable bodies. Both the cutting tool and workpiece are divided into the boundary layer, the thermostat layer, and the Newtonian layer (Figure 1). The workpiece and tool are made stable, and proper lattice symmetry is maintained during the cutting process by the boundary layer. The thermostat layer conducts away the evolved heat during the cutting process, and a Langevin thermostatic dynamics was employed (Grønbech-Jensen, 2020). Both boundary

Table 1: Simulation parameters of the cutting process

Simulation Parameters	Workpiece: Si	Diamond Tool
Number of atoms	126066	Rake angle 0^{O}, 65232
	[100],[010],[001]	atoms
	Unit lattice parameter:	Tool edge radius 3.5 nm
	5.431A	Clearance angle 10^{O}
Timestep	1fs	
Simulation temperature	293K	
Depths of cut (DoC)	4 nm, 3 nm and 2 nm	
Distance of workpiece from tool	1nm	
Cutting speed	100 m/s = 1A/ps	
Cutting direction	[-100] on (001) surface	
Potential function	Tersoff	
Run	250,000	

and thermostat layers were 1nm thick. Non-period shrink-wrapped boundary conditions were adopted in the x-direction and y-direction, while periodic boundary conditions were adopted in the z-direction because of the small size of the workpiece in this direction and to ensure that the size effect is reduced. During the simulation process, the initial temperatures of the silicon and the diamond tool were equilibrated at 293K using the Langevin method for a period of 20 ps. The thermostat and the Newtonian atoms were set into motion following the classical Newton's second law. The equation of motion was numerically integrated using the Velocity Verlet algorithm with a timestep of 1 femtosecond.

For reliable and accurate molecular dynamics simulation results, the proper choice of the potential energy function for a specific material workpiece is essential. The use of Tersoff potentials is widely employed and affirmed to be able to predict the mechanical behaviour of silicon (Tersoff, 1986; Shimada et al., 1995;Lin et al., 2007;). The Tersoff potential function is feasibly capable of dealing with elements in group IV and those with a diamond lattice structure and covalently bonded like carbon, germanium, and silicon (Tersoff, 1986, 1988, 1989). In this research, all the interactions among the atom types are described employing Tersoff potentials with parameters from elemental silicon, followed by Erhart and Able Si-II model (Erhart & Albe, 2005).

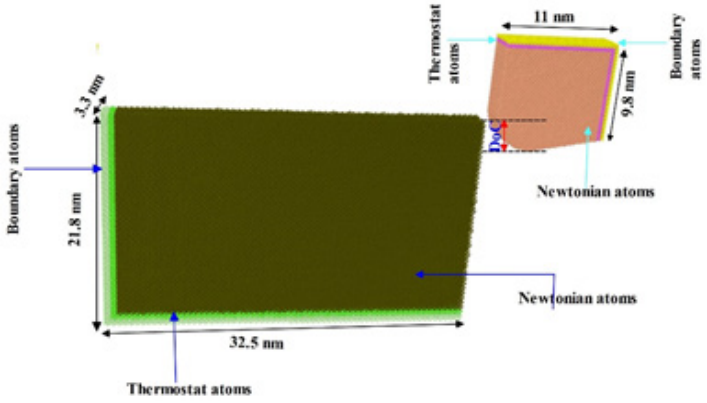

Figure 1: MD simulation model of nanometric cutting of silicon

The interaction among the atoms with the Tersoff potential function can be expressed as follows:

$$E = \frac{1}{2}\sum_{i}\sum_{j \neq i} V_{ij} \quad (1)$$

$$V_{ij} = f_C(r_{ij} + \delta)[f_R(r_{ij} + \delta) + b_{ij} f_A(r_{ij} + \delta)] \quad (2)$$

$$f_C(r) = \begin{cases} 1, r < R - D \\ \frac{1}{2} - \frac{1}{2}\sin\left[\frac{\pi}{2}\left(r - \frac{R}{2}\right)\right], R - D < r < R + D \\ 0, r > R + D \end{cases} \quad (3)$$

$$f_R(r) = Aexp(-\lambda \quad (4)$$

$$f_A(r) = -Bexp(-\lambda_2 r) \quad (5)$$

$$b_{ij} = \left(1 + \beta^n \zeta_{ij}^n\right)^{-\frac{1}{2n}} \quad (6)$$

$$\zeta_{ij} = \sum_{k \neq ij} f_C(r_{ik} + \delta) g\left[\theta_{ijk}(r_{ij}, r_{ik})\right] exp\left[\lambda_3^m (r_{ij} - r_{ik})^m\right] \quad (7)$$

$$g(\theta) = \gamma_{ijk}\left(1 + \frac{c^2}{d^2} - \frac{c^2}{[d^2 + (\cos\theta - \cos\theta_0)^2]}\right) \quad (8)$$

E is the total energy of the system, V_{ij} is the potential energy; i j and k are atoms labels of the system, r_{ij} is the length of the $i - j$ bond, b_{ij} is the bond order parameter, θ_{ijk} is the bond angle between the bonds i - j and $i - j$, f_R is a repulsive pair potential, f_A is an attractive pair potential, f_C represents a smooth cut-off function to limit the range of the potential, ζ_{ij}^n is the number of effective coordination, and R and S indicate the inclusion of the first shell neighbours.

The Archer2 HPC was used to run the molecular dynamics simulation of this study on 16 cores with the large-scale atomic/molecular massively parallel simulator (LAMMPS) molecular dynamics code (Thompson et al., 2022). The atomistic data from the simulations were analysed and visualised using Ovito (Stukowski, 2010). The atom's structural transformation and dislocation during the deformation were identified and analysed by employing the Identify Diamond Structure algorithm, coordination algorithm, and dislocation extraction algorithm (DXA) in Ovito.

3. Results and discussions

3.1. Atomic flow of the chip formation and the surface finish

The chip formation at a nanoscale is influenced by stagnation in a stagnation region. It is a region where the displacement of the atoms is smaller than one-tenth of the other atoms in the workpiece cutting direction during the cutting process (Liu et al., 2021). The atoms in this region are stagnated by the tool edge. It is reported that the stagnation region is formed infront of the tool, and the stagnation point S (Figure 2c) is a point that separates the workpiece atoms into removed chips, machined surface, and stagnation atoms (Xu et al., 2017a; Xu et al., 2017b). Atoms of higher displacement flow upwards to form chips continuously and are being removed. For elastic-plastic deformation, where no material removal is involved, atoms piled up on the rake face flow down along the tool flank face to form the machined surface (Lai et al., 2012; Xu et al., 2017a). The displacement vector algorithm in Ovito was used to obtain the atomic flow of the deformed atoms and to locate the stagnation points for depths of cut of 2 nm, 3 nm, and 4 nm (Figure 2). The region

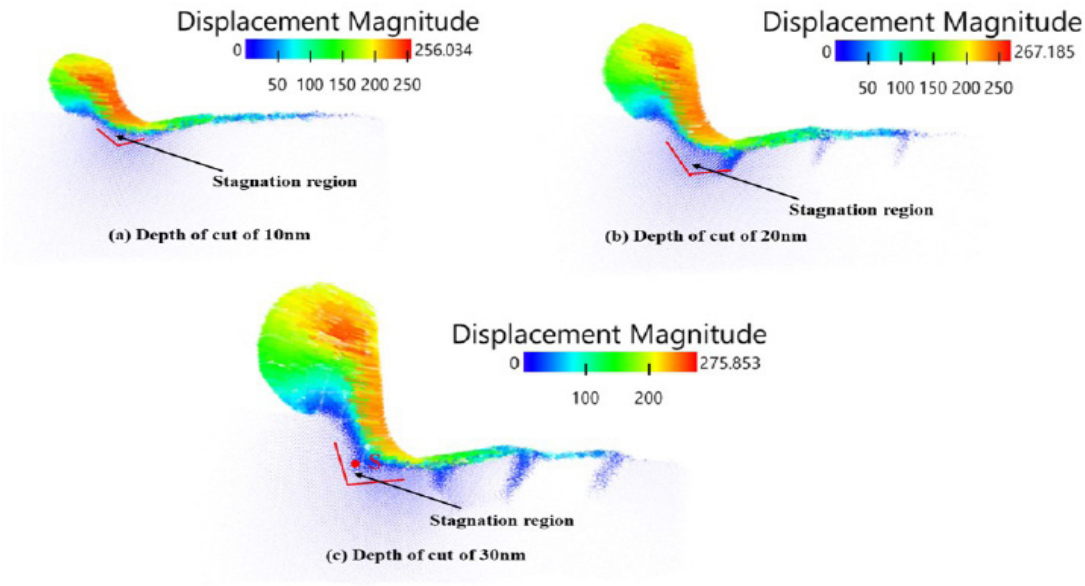

Figure 2: Schematic snapshots of the displacement vector of atomic flow at different depths of cuts.

below the tool with a displacement magnitude of around 50 angstroms is the stagnation region. The stagnation regions increase as the depths of cut increase. With the depth of cut of 4 nm, more atoms flow upwards to form chips. This is evident with the highest chip thickness, compared to the depths of cut of 2 nm and 3 nm. More atoms piled up in the rake face and flew down to form the machined surface. The depth of cut of 2 nm with a lesser stagnation region and fewer atoms flowing down to form the machined surface, and its subsurface damage layer would be less. It could be assumed that the wider the stagnation region, the longer the subsurface damage layer or the more the cutting-induced subsurface damage region would be. Apart from this, the coordination analysis carried out in this research reveals that the wider the stagnation region, the more the transformed atoms, particularly atoms with coordination numbers of 5 and 6. Xu et al. (2018) relate this observation to the stagnation height. Higher stagnation height gives a large number of phase-transformed atoms due to more materials being flown down the subsurface.

3.2. Deformation mechanisms and subsurface damage depth

The simulation models before and after the nanocutting are shown in Figure 4 using the Identify Diamond Structure algorithm in Ovito to identify crystal deformation and phase transformation. Before nano-cutting, the workpiece and the tool show a perfect diamond lattice structure (blue colour, light blue, and light green) (Figure 3a). After cutting for 25 nm, there was a structural and phase transformation of diamond lattice structures of the workpiece atoms, as indicated by atoms with grey colours (Figure 3b). The grey atoms are the deformed atoms that are transformed from the diamond cubic structure of silicon (c-Si/Si-I) to Si-II/β-Si (a 6-fold metastable phase) and 5-fold bct5-Si because of high hydrostatic pressure near the cutting edge. The coordination number analysis reveals that some bct5-Si and β-Si form the chips, and other parts of these structures form the machined surface under the cutting action of the diamond tool. Similar observations were reported by Wang et al. (2017). Under extreme localised stresses beneath the tool, the β-Si being unstable transforms to high-pressure phases Si-III and Si-XII and transforms into the a-Si phase when the pressure release rate is high (Chavoshiet al., 2016a; Chen et al., 2020; Wu et al., 2010).

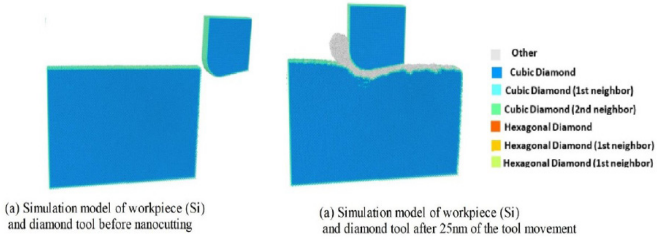

Figure 3: Snapshots of MD models of crystal structure deformation

The snapshots of the effects of depth of cuts on the deformation and phase transformation of silicon nanometric cutting are shown in Figure 4. For all the depth of cuts, the curl chips are formed: an indication of the ductile mode of cutting. The workpiece with a depth of cut of 2 nm gives a machined surface with

the least subsurface damage layer. Silicon workpiece with a depth of cut of 4 nm has the highest subsurface damage length, and the machined surface at this depth of cut has a crystallite alongside the a-Si atoms that formed the machined surface. The observation of the highest subsurface damage (SSD) length is evident from the stagnation mechanism discussed earlier because more atomic flows were pressed down to form the machined surface. The observed crystallite indicates that the deformation mechanism is no longer a pure ductile mode, but a mix of ductile-brittle due to high-pressure phase transformation and cleavage fracture. No previous investigation reports this observation with the tool geometry used, except Wang et al. (2017), who used a tool geometry of a negative rake of 7 degrees and a clearance angle of 7 degrees. Zhang et al. (2014) investigated the deformation behaviour of nanometric cutting of silicon using molecular dynamics simulation with the same tool geometry used in this investigation, but they do not report crystallites. Wang et al. (2017) observed the crystallites for both deformed atoms in both the chip and machined surface for some silicon orientations. However, it is claimed that the surface integrity of the workpiece is not much influenced by the cleavage but by the degree of SSD (Wang et al., 2017). In this investigation, the silicon workpiece with a depth of cut of 4 nm gives a machined surface with cleavage and severe SSD. This implies that cutting at this depth of cut might not be appropriate, because its value is higher than the tool cutting edge radius (3.5 nm), which will not enable ductile mode machining.

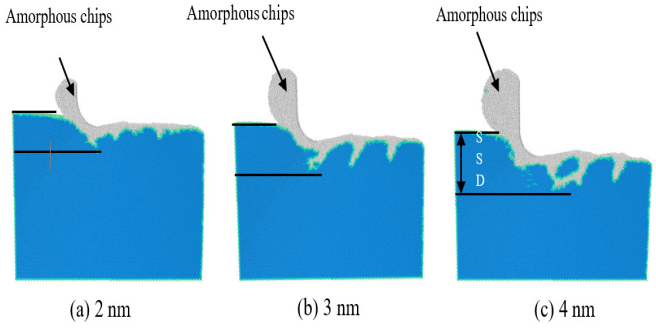

Figure 4: Chip morphology, subsurface damage, and deformation of silicon nanometric cutting

3.3. Silicon phase transformation using coordination number

Coordination analysis has been used to explain the phase transformation of the machining of various materials at the nano-scale (Liu, 2014; Lai et al., 2017; Wang et al., 2017; Fan et al., 2020). . For easy understanding of deformation and phase transformation (visualisations), atoms with a coordination number (CN) equal to 4 were deliberately removed, leaving only the deformed and phase transformation atoms (Figure 5). The atoms with CN less than 4 formed the boundary atoms. Some of these atoms are found to move along the chip surface, machined surface, and subsurface. They are described as defective cubic and hexagonal atoms, and their formation is attributed to the combined effects of subsurface dislocation activities and surface amorphisation (Wu et al., 2023). The atoms with CN above 4 play a major role in the phase transformation. These phase transformation atoms are indications of structural phase transformations of the monocrystalline silicon atoms (Zhang et al., 2014). The schematic snapshots and graphical representations of the coordination analysis are shown in Figure 5 and Figure 6 for different depths of cuts. For all depths of cuts, the atoms with CN of 6 and 5 are β-Si and bct5-Si, respectively and are responsible for the plastic deformation during the cutting. They dominate the deformation and phase transformation. This domination is due to the earlier transition pressure of around 11 and 16 GPa (Hu et al., 1986). They are more with a depth of cut of 4 nm, as indicated by the thickness of the chip (Figure 4), because the greater the depth of cut, the more they are in the cutting region (Figure 6) (Chen et al., 2018). The more of these atoms, the more the resistance to cutting, which could result in cleavage observed on the machined surface at this depth of cut. Other atom structures with CNs of 7, 8, 9, and 10 were transformed, but concentrated at the tool-edge region and in smaller numbers.

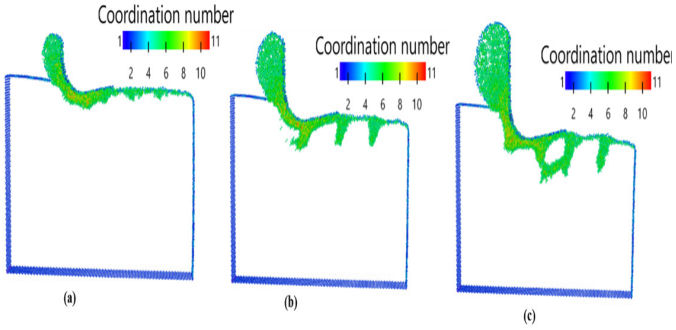

Figure 5: Snapshots of the coordination number of deformed atoms at the depth of cut of (a) 2 nm (b) 3 nm (c) 4 nm

3.4. Dislocation Distribution Observation on the Machined Surface

The machined surface after the tool moved 25nm was examined for dislocation distribution using the dislocation extraction algorithm (DXA) in Ovito. The

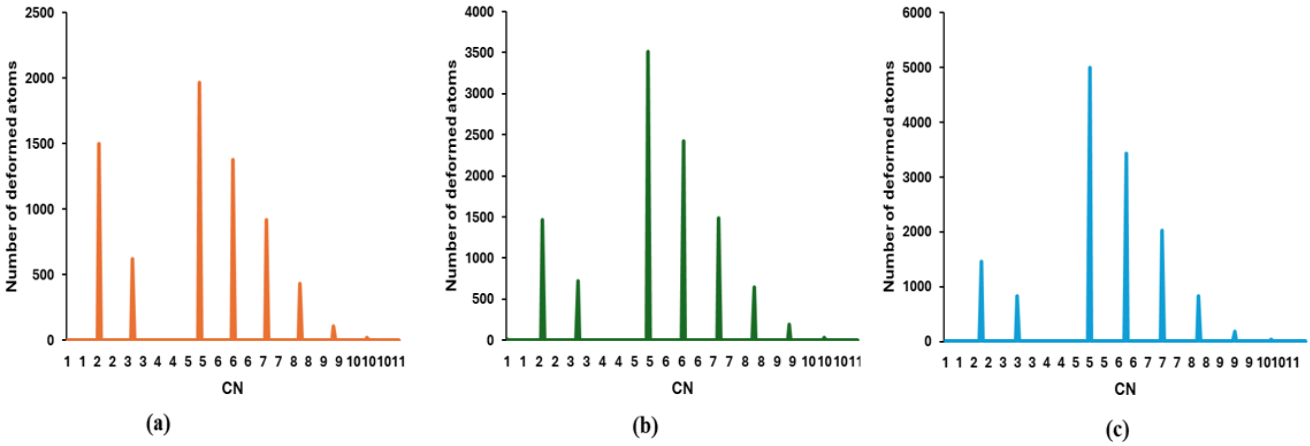

Figure 6: Deformed atoms count and corresponding coordination number at depth of cut of (a) 2 nm (b) 3 nm (c) 4 nm

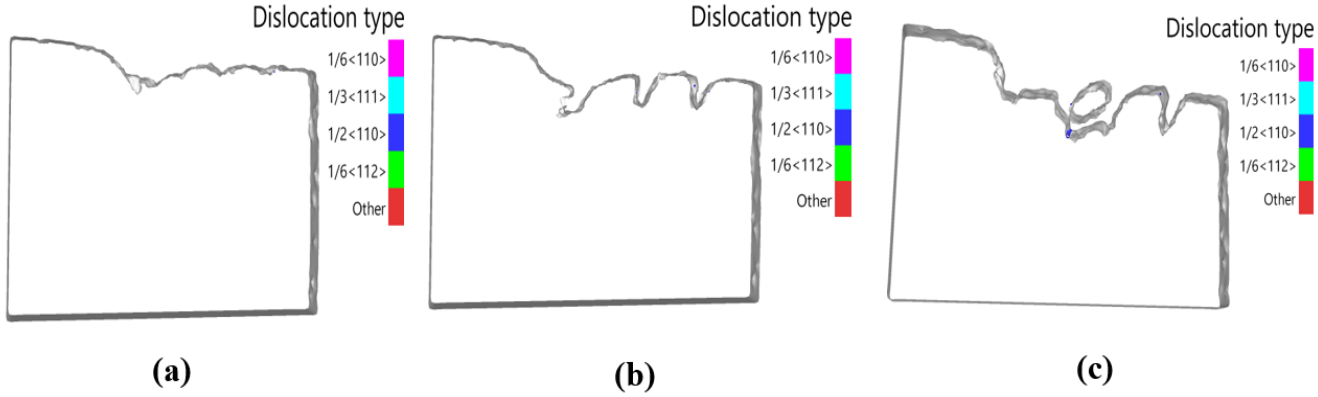

Figure 7: Dislocation distribution at the depth of cut of (a) 2 nm (b) 3 nm (c) 4 nm

snapshots are of the dislocation analysis as shown in Figure 7. No dislocation is observed for the depths of cuts of 2nm and 3nm. A perfect dislocation with a Burger vector of ½<1110> (blue colour) is observed with a depth of cut of 3nm. This implies that at this depth of cut, dislocation activities as well as phase transformation are contributors to the plastic deformation, as claimed by (Gassilloud et al., 2005; Sharma et al., 2018). It is also claimed that the level of cutting resistance corresponds to the amount of dislocation (Sharma et al., 2018). However, Cai et al. (2007) report no dislocation for the nanometric cutting of silicon, and that the plastic deformation of silicon is through high-pressure phase transformation.

4. Conclusion and recommendation

The deformation and material removal mechanisms of nanometric cutting of silicon under different depths of cut were analysed by examining the chip formation mechanism, phase transformation, and dislocation. It is established that the structural and phase transformation of silicon is due to high-pressure phase transformation, and dislocation action at a deeper depth of cut (4 nm) leads to chip formation and a machined surface. For all depths of cuts, the material removal mechanism was ductile mode machining, except for a depth of cut of 4 nm, which exhibited a mix of ductile and cleavage behaviour, as revealed by the crystallites formed on the machined surface. To ensure a ductile mode of machining with this tool geometry, the depth of cut should be much smaller than the cutting-edge radius of the diamond tool.

References

Agarwal, S., Khare, S. Kr., Pandey, V. P., & Patel, M. (2017) An Analytical Chip Thickness Model for Performance Assessment in Silicon Carbide Grinding. *Procedia Manufacturing*, *10*, 298–306. https://doi.org/10.1016/j.promfg.2017.07.060

Arif, M., Xinquan, Z., Rahman, M., & Kumar, S. (2013) A predictive model of the critical undeformed chip thickness for ductile–brittle transition in nano-machining of brittle materials. *International Journal of Machine Tools and Manufacture*, *64*, 114–122. https://doi.org/10.1016/j.ijmachtools.2012.08.005

Bifano, T. G., Dow, T. A., & Scattergood, R. O. (1991) Ductile-Regime Grinding: A New Technology for Machining

Brittle Materials. *Journal of Engineering for Industry*, *113*(2), 184–189. https://doi.org/10.1115/1.2899676

Cai, M. B., Li, X. P., & Rahman, M. (2007) High-pressure phase transformation as the mechanism of ductile chip formation in nanoscale cutting of silicon wafer. *Proceedings of the Institution of Mechanical Engineers, Part B: Journal of Engineering Manufacture*, *221*(10), 1511–1519. https://doi.org/10.1243/09544054JEM901

Chavoshi, S. Z., Goel, S., & Luo, X. (2016a) Influence of temperature on the anisotropic cutting behaviour of single crystal silicon: A molecular dynamics simulation investigation. *Journal of Manufacturing Processes*, *23*, 201–210. https://doi.org/10.1016/j.jmapro.2016.06.009

Chavoshi, S. Z., Xu, S., & Luo, X. (2016b) Dislocation-mediated plasticity in silicon during nanometric cutting: A molecular dynamics simulation study. *Materials Science in Semiconductor Processing*, *51*, 60–70. https://doi.org/10.1016/j.mssp.2016.05.003

Chen, P., Zhang, Z., An, T., Yu, H., & Qin, F. (2018) Generation and distribution of residual stress during nano-grinding of monocrystalline silicon. *Japanese Journal of Applied Physics*, *57*, 121302. https://doi.org/10.7567/JJAP.57.121302

Chen, X., Liu, C., Ke, J., Zhang, J., Shu, X., & Xu, J. (2020) Subsurface damage and phase transformation in laser-assisted nanometric cutting of single crystal silicon. *Materials and Design*, *190*. Scopus. https://doi.org/10.1016/j.matdes.2020.108524

Cheng, K., Luo, X., Ward, R., & Holt, R. (2003) Modeling and simulation of the tool wear in nanometric cutting. *Wear*, *255*(7), 1427–1432.

Davies, M. A., Evans, C. J., Vohra, R. R., Bergner, B. C., & Patterson, S. R. (2003) Application of precision diamond machining to the manufacture of microphotonics components. *Lithographic and Micromachining Techniques for Optical Component Fabrication II*, *5183*, 94–109. https://doi.org/10.1117/12.506373

Ebizuka, N., Dai, Y., Eto, H., Lin, W., Ebisuzaki, T., Omori, H., Handa, T., Takami, H., & Takahashi, Y. (2003) Development of SiC ultra light mirror for large space telescope and for extremely huge ground based telescope. *Specialized Optical Developments in Astronomy*, *4842*, 329–334.

Erhart, P., & Albe, K. (2005) Analytical potential for atomistic simulations of silicon, carbon, and silicon carbide. *Physical Review B*, *71*(3), 035211. https://doi.org/10.1103/PhysRevB.71.035211

Fan, P., Goel, S., Luo, X., Yan, Y., Geng, Y., & Wang, Y. (2020) An atomistic investigation on the wear of diamond during atomic force microscope tip- based nanomachining of Gallium Arsenide. *Computational Materials Science*, *187*. https://doi.org/10.1016/j.commatsci.2020.110115

Feng, R., Qi, Y., Zhu, Z., Song, W., Li, H., Wang, M., Rui, Z., & Gu, F. (2020) Molecular Dynamics Simulation to Investigate the Rake Angle Effects on Nanometric Cutting of Single Crystal Ni3Al. *International Journal of Precision Engineering and Manufacturing*, *21*(4), 711–724. https://doi.org/10.1007/s12541-019-00249-z

Gassilloud, R., Ballif, C., Gasser, P., Bürki, G., & Michler, J. (2005) Deformation mechanisms of silicon during nanoscratching. *Physica Status Solidi (a)*, *202*. https://doi.org/10.1002/pssa.200521259

Goel, S. (2013) *An atomistic investigation on the nanometric cutting mechanism of hard, brittle materials* [PhD Thesis]. Heriot-Watt University.

Grønbech-Jensen, N. (2020) Complete set of stochastic Verlet-type thermostats for correct Langevin simulations. *Molecular Physics*, *118*(8), e1662506. https://doi.org/10.1080/00268976.2019.1662506

Hu, J. Z., Merkle, L. D., Menoni, C. S., & Spain, I. L. (1986) Crystal data for high-pressure phases of silicon. *Physical Review B*, *34*(7), 4679–4684. https://doi.org/10.1103/PhysRevB.34.4679

Ikawa, N., Donaldson, R. R., Komanduri, R., König, W., McKeown, P. A., Moriwaki, T., & Stowers, I. F. (1991a) Ultraprecision metal cutting—The past, the present and the future. *CIRP Annals-Manufacturing Technology*, *40*(2), 587–594.

Ikawa, N., Shimada, Sh., Tanaka, H., & Ohmori, G. (1991b) An Atomistic Analysis of Nanometric Chip Removal as Affected by Tool-Work Interaction in Diamond Turning. *CIRP Annals*, *40*(1), 551–554. https://doi.org/10.1016/S0007-8506(07)62051-4

Komanduri, R., & Raff, L. M. (2001) A review on the molecular dynamics simulation of machining at the atomic scale. *Proceedings of the Institution of Mechanical Engineers, Part B: Journal of Engineering Manufacture*, *215*(12), 1639–1672. https://doi.org/10.1177/095440540121501201

Lai, M., Zhang, X., & Fang, F. (2012) Study on critical rake angle in nanometric cutting. *Applied Physics A*, *108*. https://doi.org/10.1007/s00339-012-6973-8

Lai, M., Zhang, X., & Fang, F. (2017) Crystal orientation effect on the subsurface deformation of monocrystalline germanium in nanometric cutting. *Nanoscale Research Letters*, *12*, 1–10.

Lin, Y.-H., Chen, T.-C., Yang, P.-F., Jian, S.-R., & Lai, Y.-S. (2007) Atomic-level simulations of nanoindentation-induced phase transformation in mono-crystalline silicon. *Applied Surface Science*, *254*(5), 1415–1422. https://doi.org/10.1016/j.apsusc.2007.06.071

Liu, C., Chu, J., Zhang, J., Zhang, J., Chen, X., Xiao, J., & Xu, J. (2021) Effect of tool rake angle on the material removal mechanism transition of single-crystal silicon: A molecular dynamics study. *The International Journal of Advanced Manufacturing Technology*, *115*(11), 3631–3644. https://doi.org/10.1007/s00170-021-07391-x

Liu, M. (2014) Crystal plasticity and experimental studies of nano-indentation of aluminium and copper. *University of Wollongong Thesis Collection 1954-2016*. https://ro.uow.edu.au/theses/4219

Maekawa, K., & Itoh, A. (1995) Friction and tool wear in nano-scale machining—A molecular dynamics approach. *Wear*, *188*(1–2), 115–122. https://doi.org/10.1016/0043-1648(95)06633-0

Neo, W., Kumar, A., & Rahman, M. (2012) A review on the current research trends in ductile regime machining. *International Journal of Advanced Manufacturing Technology*, *63*(5–8), 465–480. https://doi.org/10.1007/s00170-012-3949-y

Ngoi, B. K. A., & Sreejith, P. S. (2000) Ductile Regime Finish Machining—A Review. *The International Journal of Advanced Manufacturing Technology*, *16*(8), 547–550. https://doi.org/10.1007/s001700070043

Ravindra, D., Ghantasala, M. K., & Patten, J. (2012) Ductile mode material removal and high-pressure phase transformation in silicon during micro-laser assisted machining. *Precision Engineering*, *36*(2), 364–367. https://doi.org/10.1016/j.precisioneng.2011.12.003

Sharma, A., Datta, D., & Balasubramaniam, R. (2018) Molecular dynamics simulation to investigate the orientation effects on nanoscale cutting of single crystal copper. *Computational Materials Science*, *153*, 241–250. https://doi.org/10.1016/j.commatsci.2018.07.002

Shimada, S., Ikawa, N., Inamura, T., Takezawa, N., Ohmori, H., & Sata, T. (1995) Brittle-Ductile Transition Phenomena in Microindentation and Micromachining. *CIRP Annals*, *44*(1), 523–526. https://doi.org/10.1016/S0007-8506(07)62377-4

Shore, P., & Morantz, P. (2012) Ultra-precision: Enabling our future. *Phil. Trans. R. Soc. A*, *370*(1973), 3993–4014. https://doi.org/10.1098/rsta.2011.0638

Stukowski, A. (2010) Visualization and analysis of atomistic simulation data with OVITO-the Open Visualization Tool. *Modelling and Simulation in Materials Science and Engineering*, *18*. https://doi.org/10.1088/0965-0393/18/1/015012

Taniguchi, N. (1983) Current Status in, and Future Trends of, Ultraprecision Machining and Ultrafine Materials Processing. *CIRP Annals*, *32*(2), 573–582. https://doi.org/10.1016/S0007-8506(07)60185-1

Tersoff, J. (1986) New empirical model for the structural properties of silicon. *Physical Review Letters*, *56*(6), 632–635. Scopus. https://doi.org/10.1103/PhysRevLett.56.632

Tersoff, J. (1988) Empirical interatomic potential for silicon with improved elastic properties. *Physical Review B*, *38*(14), 9902–9905. https://doi.org/10.1103/PhysRevB.38.9902

Tersoff, J. (1989) Modeling solid-state chemistry: Interatomic potentials for multicomponent systems. *Physical Review B*, *39*(8), 5566–5568. https://doi.org/10.1103/PhysRevB.39.5566

Thompson, A. P., Aktulga, H. M., Berger, R., Bolintineanu, D. S., Brown, W. M., Crozier, P. S., In 'T Veld, P. J., Kohlmeyer, A., Moore, S. G., Nguyen, T. D., Shan, R., Stevens, M. J., Tranchida, J., Trott, C., & Plimpton, S. J. (2022) LAMMPS - a flexible simulation tool for particle-based materials modeling at the atomic, meso, and continuum scales. *Computer Physics Communications*, *271*, 108171. https://doi.org/10.1016/j.cpc.2021.108171

Venkatachalam, S. (2007) *Predictive modeling for ductile machining of brittle materials*. Georgia Institute of Technology.

Wang, Z., Chen, J., Wang, G., Bai, Q., & Liang, Y. (2017). Anisotropy of Single-Crystal Silicon in Nanometric Cutting. *Nanoscale Research Letters*, *12*. https://doi.org/10.1186/s11671-017-2046-4

Wu, Y. Q., Huang, H., Zou, J., Zhang, L. C., & Dell, J. M. (2010) Nanoscratch-induced phase transformation of monocrystalline Si. *Scripta Materialia*, *63*(8), 847–850. https://doi.org/10.1016/j.scriptamat.2010.06.034

Wu, Z., Zhang, L., Yang, S., Wu, C., Xu, K., & Zheng, D. (2023) Effects of temperature on the deformation of 6H–SiC during nanoscratching. *Wear*, *523*, 204843. https://doi.org/10.1016/j.wear.2023.204843

Xu, F., Fang, F., & Zhang, X. (2017a) Side Flow Effect on Surface Generation in Nano Cutting. *Nanoscale Research Letters*, *12*(1), 359. https://doi.org/10.1186/s11671-017-2136-3

Xu, F., Wang, J., Fang, F., & Zhang, X. (2017b) A study on the tool edge geometry effect on nano-cutting. *The International Journal of Advanced Manufacturing Technology*, *91*(5), 2787–2797. https://doi.org/10.1007/s00170-016-9922-4

Xu, F., Fang, F., & Zhang, X. (2018) Effects of recovery and side flow on surface generation in nano-cutting of single crystal silicon. *Computational Materials Science*, *143*, 133–142. https://doi.org/10.1016/j.commatsci.2017.11.002

Zhang, L., Zhao, H., Yang, Y., Huang, H., Ma, Z., & Shao, M. (2014) Evaluation of repeated single-point diamond turning on the deformation behavior of monocrystalline silicon via molecular dynamic simulations. *Applied Physics A*, *116*(1), 141–150. https://doi.org/10.1007/s00339-014-8243-4

Zhang, Z., Chen, P., Qin, F., An, T., & Yu, H. (2018) Mechanical properties of silicon in subsurface damage layer from nano-grinding studied by atomistic simulation. *AIP Advances*, *8*(5), 055223. https://doi.org/10.1063/1.5021654